

High-fidelity, high-isotropic resolution diffusion imaging through gSlider acquisition with B_1^+ & T_1 corrections and multi-coil B_0 shim array

Congyu Liao^{1,2}, Jason Stockmann^{1,2}, Qiyuan Tian^{1,2}, Berkin Bilgic^{1,2}, Mary Kate Manhard^{1,2}
Lawrence L Wald^{1,2}, and Kawin Setsompop^{1,2}

¹ Athinoula A. Martinos Center for Biomedical Imaging, Massachusetts General Hospital, Charlestown, MA, USA.

² Department of Radiology, Harvard Medical School, Charlestown, MA, USA

Synopsis

gSlider is an SNR-efficient simultaneous multi-slab acquisition that has shown great potential for high-resolution diffusion imaging (DI). In this work, approaches to improve the fidelity of gSlider are proposed. A modified reconstruction which incorporates B_1^+ inhomogeneity and T_1 recovery information was developed and demonstrated to successfully mitigate slab-boundary artifacts in short-TR gSlider acquisitions. Slice-by-slice B_0 -shimming through multi-coil shim-array, and high in-plane acceleration through virtual-coil GRAPPA were also incorporated into the acquisition and demonstrated to achieve 8-11x reduction in B_0 distortion in single-shot EPI. The modified gSlider acquisition/reconstruction was used to acquire high-fidelity whole-brain 1mm isotropic DI with 64 diffusion-directions in 20-minutes at 3T.

Introduction

High resolution diffusion imaging (DI) is limited by low-SNR. Generalized slice dithered enhanced resolution (gSlider) is an SNR-efficient acquisition technique with self-navigated RF slab-encoding, which has shown great potential for high resolution DI (1). In this work, we developed approaches to improve the fidelity of gSlider; to make it robust to slab-boundary artifacts, and to drastically reduce distortion from B_0 inhomogeneity. To mitigate slab-boundary artifacts in short-TR acquisitions, a dictionary-based B_1^+ -inhomogeneity and T_1 -recovery correction is incorporated into gSlider reconstruction. To mitigate image distortions, a 32-channel integrated $\Delta B_0/R_x$ array (AC/DC coil) (2) is utilized for slice-by-slice shimming, to reduce B_0 -inhomogeneity by >50%. This is then combined with high in-plane acceleration ($R_{\text{inplane}}=4$) and virtual conjugate coil (VCC-) GRAPPA reconstruction(3,4), to achieve 8-11x distortion reduction in single-shot gSlider-EPI. We demonstrated that the proposed method can achieve high-fidelity whole-brain 1mm-isotropic DI with 64 diffusion-directions in **20 minutes** on a 3T scanner.

Methods

Figure1(a) shows the sequence diagram of gSlider, where two external triggers are added in each TR to enable slice-by-slice B_0 -shimming with the AC/DC coil (Fig1(b)). To avoid poor performance in whole-brain fat suppression from large out-of-slice B_0 -inhomogeneity, the slice-by-slice shimming is turned off during fat saturation. In each TR, an additional k_y blip is

added to shift k-space and create more unique source points for improved VCC-GRAPPA reconstruction (4). To implement slice-optimized shimming, a field-map with conventional global-shim is acquired. Based on shim optimization on this field-map, the shim-arrays generate slice-specific DC currents for dynamic updating. For simultaneous multi-slice acquisition, the simultaneously acquired slices are shimmed jointly.

To mitigate slab-boundary artifacts, RF-encoding imperfections due to B_1^+ -inhomogeneity and incomplete T_1 -recovery are estimated and incorporated into the RF-encoding matrix (forward model) of the gSlider reconstruction. Figure 2(a) shows the flowchart of B_1^+ -inhomogeneity correction, where RF-encoding profiles at a range of flip-angles are Bloch simulated and assigned to different spatial locations represented within the RF-encoding matrix (5) using a discretized B_1^+ map. For incomplete T_1 -recovery, non-ideal slab-profiles of RF-encodings can cause partial excitations in adjacent slabs which are not fully-recovered in slab-interleaved acquisitions with short-TRs. This effect is also modeled into the Bloch simulation of the RF-encodings (assuming average $T_1=1000\text{ms}$), and incorporated into the encoding matrix. Figure 2(c) shows the partial M_z -recovery from adjacent slabs excitations before and after $TR/2$ longitudinal-relaxation at various B_1^+ excitation levels.

Acquisition: the following data were acquired using a Siemens Prisma 3T-Scanner with a custom AC/DC array:

i) To validate slice-optimized shimming, gSlider-EPI with 5 slab-encodings were acquired: FOV: $220 \times 220 \times 160 \text{mm}^3$, 32 thin-slabs (5mm slab-encoding), $TR/TE=5100/77\text{ms}$, echo spacing=0.93ms. To assess distortion, data were acquired using both Anterior-to-Posterior (AP) and Posterior-to-Anterior (PA) phase-encodings at different R_{inplane} accelerations, with and without slice-optimized shimming. A matching T_2 -SPACE data was also acquired as a distortion-free reference.

ii) whole-brain gSlider-EPI with dynamic shimming: 1mm isotropic with 64 diffusion-directions, $MB \times R_{\text{inplane}} \times \text{gSlider} = 2 \times 4 \times 5$, FOV: $220 \times 220 \times 160 \text{mm}^3$, $b=1000 \text{s/mm}^2$, $TR/TE=3500/77\text{ms}$, $T_{\text{acq}}=20\text{min}$.

B_1^+ and B_0 maps were obtained at 2mm in-plane resolution. B_1^+ map was acquired using Turbo-FLASH with 4mm slice-thickness and 25% gap. B_0 map was acquired using multi-echo GRE with 2.5mm slice-thickness and 100% gap. The slice resolution including gap for both matches the 5mm gSlider slab-encoding.

Reconstruction and post-processing: VCC-GRAPPA with phase-matching (4) was used for parallel imaging reconstruction. The 5 RF-encoded volumes of each diffusion-direction were then combined to create 1mm isotropic data, using gSlider reconstruction with proposed modified RF-encoding matrix. The data were then motion&eddy-current corrected, and averaged-DWI and FA-maps generated using FSL toolbox(6).

Results

Figure2(c) shows the B_1^+ and T_1 corrections in gSlider reconstruction, where slab-boundary artifacts are well mitigated for a short-TR acquisition at 3.5s. Figure3 show comparisons of the image distortion, with and without dynamic-shimming. The green arrows highlight the distortions that were alleviated, with slice-by-slice shimming achieving >50% reduction in ΔB_0 . This shimming is then combined with $R_{\text{inplane}}=4$ to achieve 8-11x reduction in ΔB_0 distortion, to create images with outlines closely matching that of T_2 -SPACE. Figure4(a&b) shows the B_0 -field from MB=2 dynamic shimming, where two *distant* slices are shimmed jointly, providing similar performance to the MB=1 case. Figure 5 shows averaged-DWIs and FA-maps of the 1mm isotropic DI data. High-quality results are shown, with minimal distortions even in the typically problematic areas of temporal and frontal lobes (Figure 5(c)).

Discussion and conclusion

In this work, we developed approaches to improve gSlider acquisition where i) reconstruction with B_1^+ and T_1 corrections effectively mitigate slab-boundary artifacts in short-TR acquisitions, and ii) slice-by-slice shimming and high in-plane acceleration achieve 8-11x reduction in B_0 -distortion. The proposed corrections and local-field control were used to acquire high-quality, high-fidelity DI at 1mm isotropic in 20 minutes.

Acknowledgement

This work was supported in part by NIH research grants: R01 MH116173, R01EB020613, U01EB025162, P41EB015896, and the shared instrumentation grants: S1ORR023401, S1ORR019307, S1ORR019254, S1ORR023043

References

1. Setsompop K, Fan Q, Stockmann J, et al. High-resolution in vivo diffusion imaging of the human brain with generalized slice dithered enhanced resolution: Simultaneous multislice (gSlider-SMS). *Magn. Reson. Med.* 2018;79:141–151. doi: 10.1002/mrm.26653.
2. Stockmann JP, Witzel T, Keil B, Polimeni JR, Mareyam A, Lapierre C, Setsompop K, Wald LL. A 32-channel combined RF and B0shim array for 3T brain imaging. *Magn. Reson. Med.* 2016;75:441–451. doi: 10.1002/mrm.25587.
3. Blaimer M, Gutberlet M, Kellman P, Breuer FA, Köstler H, Griswold MA. Virtual coil concept for improved parallel MRI employing conjugate symmetric signals. *Magn. Reson. Med.* 2009;61:93–102. doi: 10.1002/mrm.21652.
4. Liao C, Manhard MK, Bilgic B, et al. Joint Virtual Coil Reconstruction with Background Phase Matching for Highly Accelerated Diffusion Echo-Planar Imaging. In: ISMRM . Paris; 2018. p. 0465.
5. Pauly J, Le Roux P, Nishimura D, Macovski A. Parameter relations for the Shinnar-Le Roux selective excitation pulse design algorithm (NMR imaging). *IEEE Trans. Med. Imaging* 1991;10:53–65. doi: 10.1109/42.75611.

6. Jenkinson M, Beckmann CF, Behrens TEJ, Woolrich MW, Smith SM. Fsl. *Neuroimage* 2012;62:782–790. doi: 10.1016/j.neuroimage.2011.09.015.

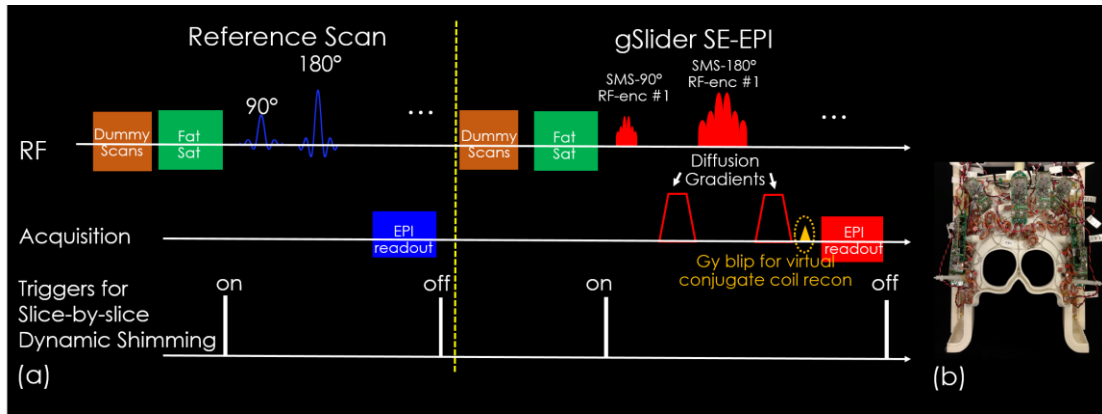


Figure 1. (a) sequence diagram of gSlider acquisition and (b) the 32-channel combined RF and B0 shim array.

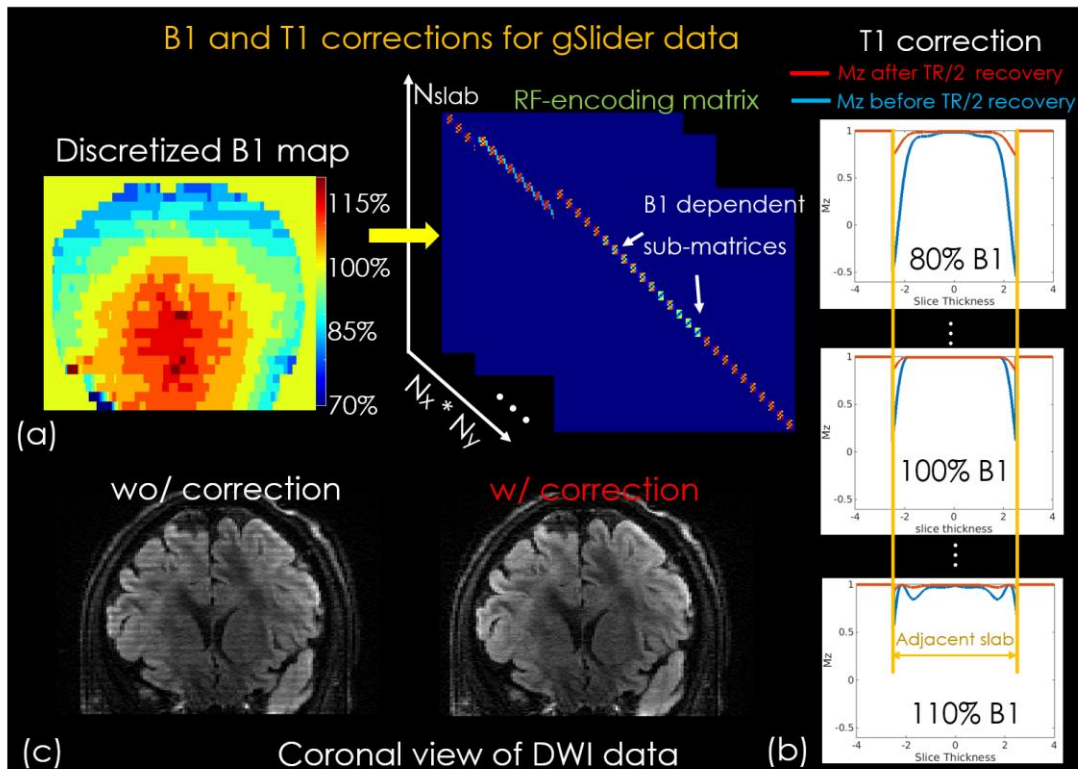


Figure 2. The flowchart of (a) B1⁺ inhomogeneity and (b) T1 corrections for gSlider data. (c) the results with and without correction.

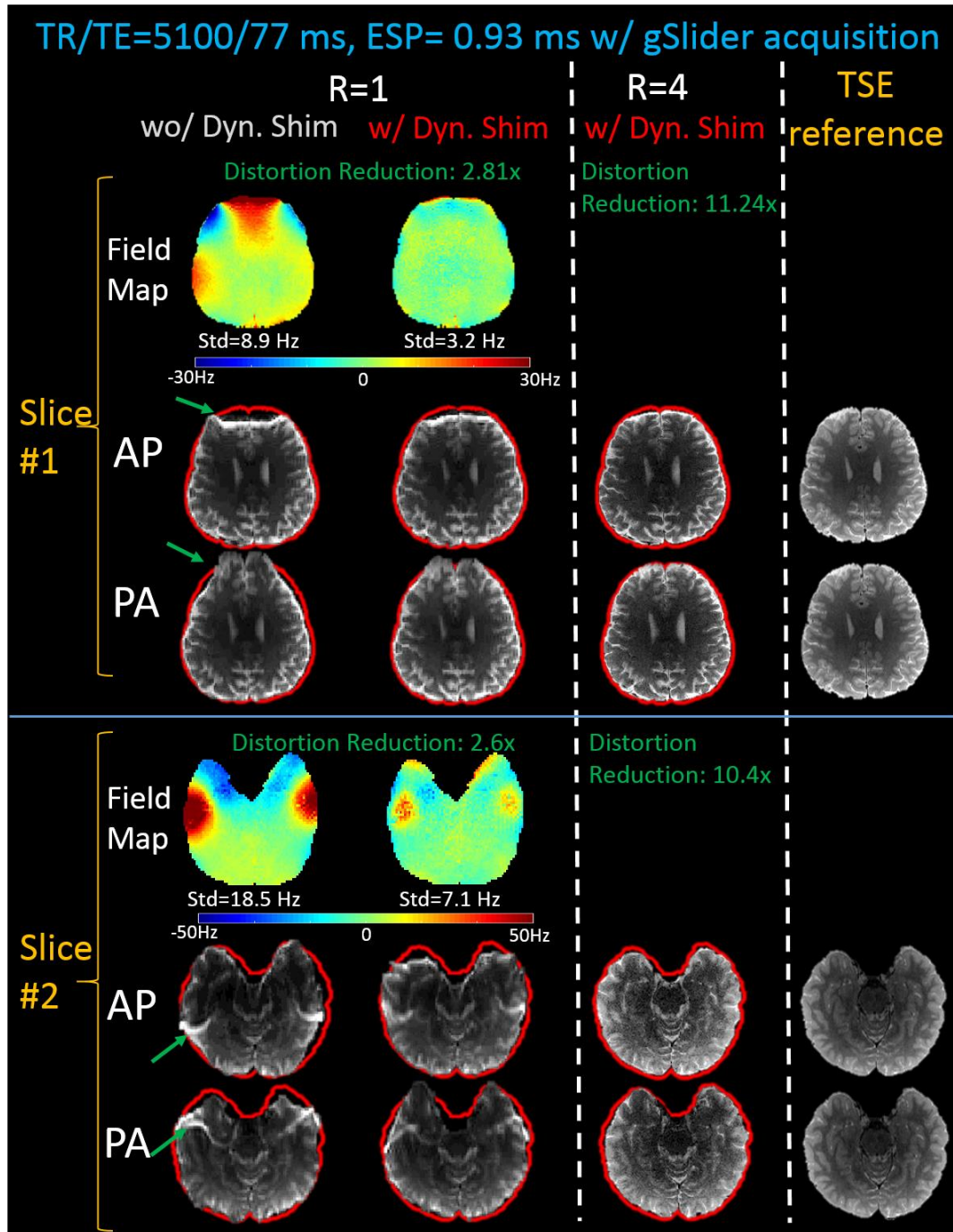


Figure 3. The comparisons of the field maps and EPI distortions with Anterior-to-Posterior (AP) and Posterior-to-Anterior (PA) phase-encodings, with and without dynamic shimming. The shimming is then combined with $R_{inplane4}$ acceleration to achieve ~ 10 -fold reduction in EPI distortion, and create low-distortion images. The red outlines shows the contour of T2-SPACE reference.

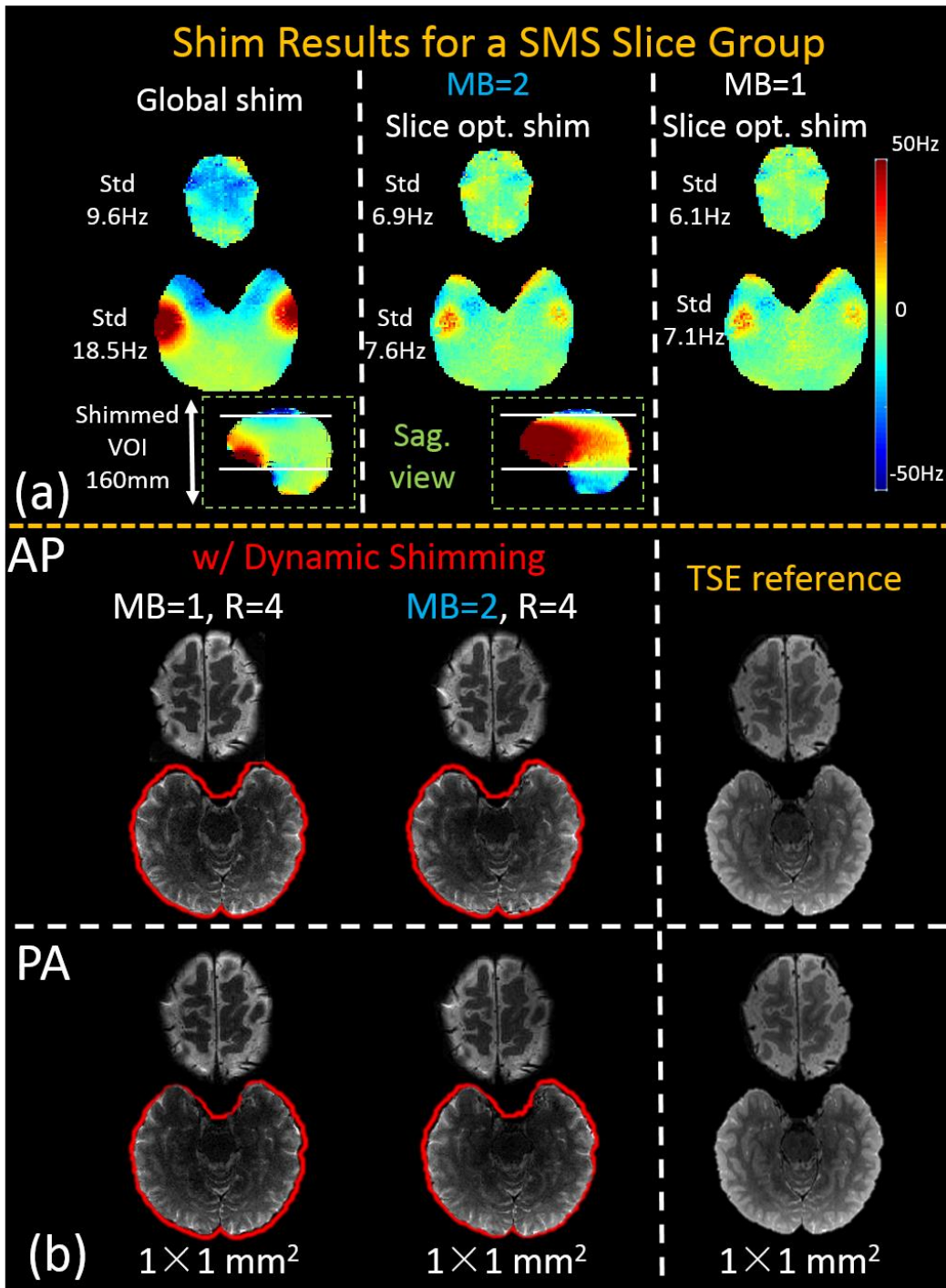


Figure 4. The shim results for a SMS slice group. (a) compared to global shim, in MB=2 case, the two distant slices are shimmed jointly, while out-of-slices regions are unconstrained and are allowed to have poor shim. The MB=2 shimming performance closely resembles that of the MB=1 slice-optimized shimming, as shown in (b).

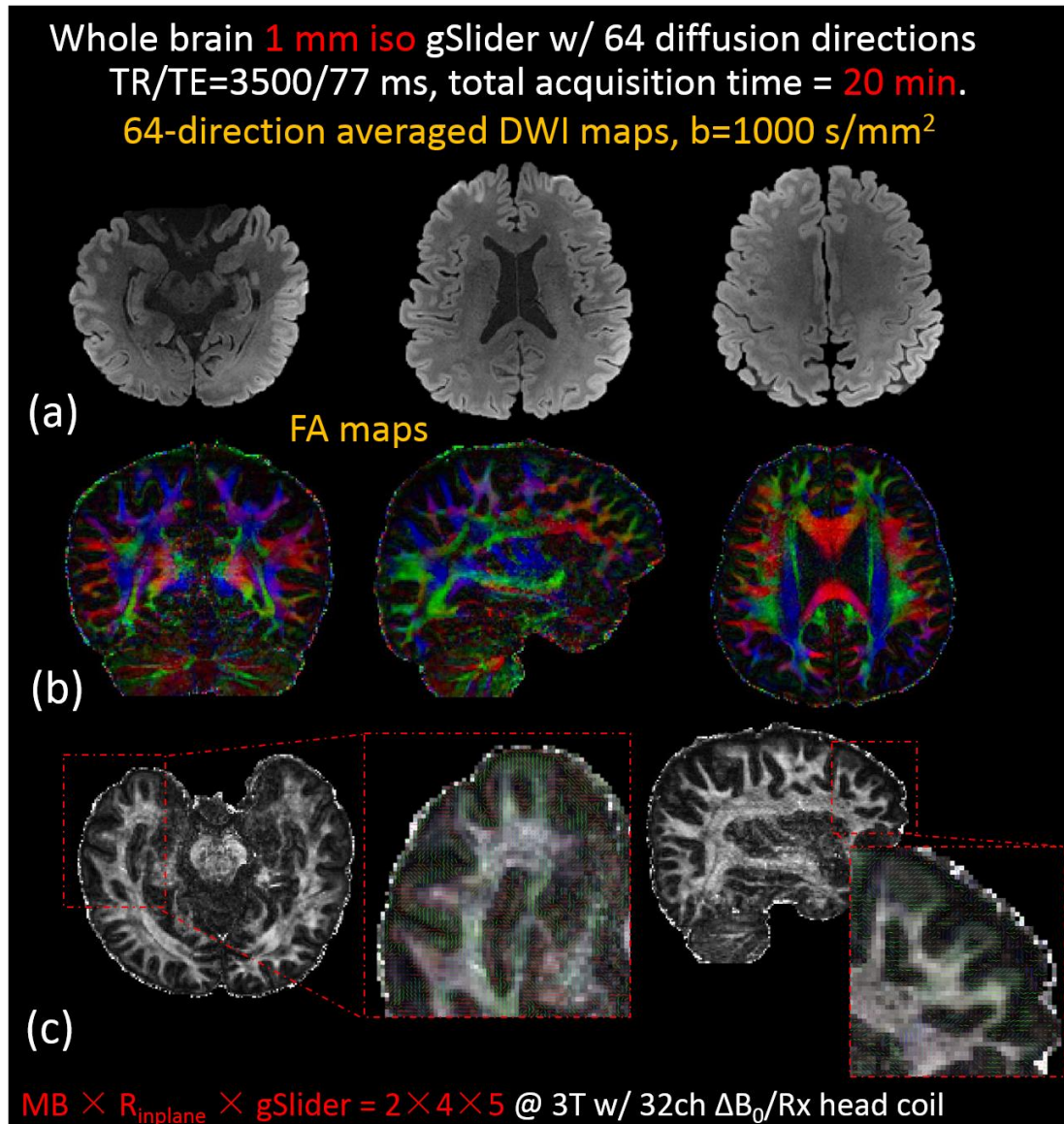


Figure 5. (a) the averaged-DWIs and (b, c) FA maps of the 1 mm isotropic DI data with 64 directions obtained in just **~20-minutes** using the proposed correction and dynamic shimming framework. (c) The typically problematic areas of the temporal and frontal lobes of the brain can be observed by using dynamic shimming.